The American Journal of Pathology, Vol. 172, No. 5, May 2008

DOI: 10.2353/ajpath.2008.071068

Epithelial and Mesenchymal Cell Biology

Absence of αvβ6 Integrin Is Linked to Initiation and Progression of Periodontal Disease

Farzin Ghannad,* Daniela Nica,* Maria I. Garcia Fulle,* Daniel Grenier,† Edward E. Putnins,* Sarah Johnston,* Ameneh Eslami,* Leeni Koivisto,* Guoqiao Jiang,* Marc D. McKee,‡ Lari Häkkinen,* and Hannu Larjava*

From the Laboratory of Periodontal Biology, Faculty of Dentistry, University of British Columbia, Vancouver; the Faculty of Dentistry and Medicine,† University of Laval, Montreal; and the Faculty of Dentistry and Department of Anatomy and Cell Biology,‡ McGill University, Montreal, Canada*

Integrin αvβ6 is generally not expressed in adult epithelia but is induced in wound healing, cancer, and certain fibrotic disorders. Despite this generalized absence, we observed that αvβ6 integrin is constitutively expressed in the healthy junctional epithelium linking the gingiva to tooth enamel. Moreover, expression of αvβ6 integrin was down-regulated in human periodontal disease, a common medical condition causing tooth loss and also contributing to the development of cardiovascular diseases by increasing the total systemic inflammatory burden. Remarkably, integrin β6 knockout mice developed classic signs of spontaneous, chronic periodontal disease with characteristic inflammation, epithelial down-growth, pocket formation, and bone loss around the teeth. Integrin αvβ6 acts as a major activator of transforming growth factor-β1 (TGF-β1), a key anti-inflammatory regulator in the immune system. Co-expression of TGF-β1 and αvβ6 integrin was observed in the healthy junctional epithelium. Moreover, an antibody that blocks αvβ6 integrin-mediated activation of TGF-β1 initiated inflammatory periodontal disease in a rat model of gingival inflammation. Thus, αvβ6 integrin is constitutively expressed in the epithelium sealing the gingiva to the tooth and plays a central role in protection against inflammatory periodontal disease through activation of TGF-β1. ***(Am J Pathol 2008, 172:1271–1286; DOI: 10.2353/ajpath.2008.071068)***

Integrin αvβ6 is an exclusively epithelial receptor that is expressed during tissue development but is absent from normal healthy epidermis and oral mucosa.[1] Expression of αvβ6 integrin is induced in wound keratinocytes of epidermis and oral mucosa, in cancer, and under certain inflammatory conditions.[2–5] Integrin β6 subunit pairs exclusively with αv subunit, and the elimination of the β6 subunit leads specifically to αvβ6 integrin deficiency. Inactivation of the β6 integrin gene results in mild inflammatory changes in the skin and lungs.[6] These changes are associated with altered signaling of transforming growth factor-β1 (TGF-β1).

TGF-β1 belongs to a family of polypeptides that has multiple regulatory functions in tissue repair and the immune system.[7,8] It is secreted from cells as a latent precursor complex, consisting of the mature dimeric growth factor, the latency-associated propeptide (LAP), and latent TGF-β1-binding protein (LTBP1). The secreted latent TGF-β1 complex is bound to the extracellular matrix via LTBP1,[9] and LTBP1 plays a role in its activation.[10–12] The activation and release of latent TGF-β1 is a complex process involving conformational changes that can be introduced by many mechanisms, including proteolytic cleavage of LAP by plasmin, thrombin, matrix metalloproteinases (MMPs), or endoglycosidases, cross-linking by transglutaminase, steroids, or active oxygen species, or binding to thrombospondin-1 (TSP-1) or αvβ6 integrin. In the αvβ6 integrin-mediated activation of TGF-β1, αvβ6 integrin binds to the RGD sequence of LAP in the extracellular matrix-bound latent TGF-β1 complex.[13,14] This binding generates a retractile force leading to a conformational change in LAP and a subsequent release of active TGF-β1.[14]

Small basal levels of TGF-β1 expression had been found in keratinocytes in normal mouse and human epidermis, where it acts as an anti-proliferative agent.[15,16] Inhibition of epithelial cell proliferation by TGF-β1 involves up-regulation of cyclin-dependent kinase inhibitors p15 and p21.[17,18] One of the most recognized functions of TGF-β1 is, however, in immunoregulation.[19,20] This is evidenced by the fact that TGF-β1-knockout mice die a few weeks after birth from massive infiltration of lymphocytes and macrophages in many organs.[21,22] TGF-β1 acts as an anti-inflammatory agent through its

Supported by the Canadian Institutes of Health Research (grant MOP-12589).

Accepted for publication February 7, 2008.

Address reprint requests to Dr. Hannu Larjava, University of British Columbia, Faculty of Dentistry, Laboratory of Periodontal Biology, 2199 Wesbrook Mall, Vancouver, BC, Canada V6T 1Z3. E-mail: larjava@interchange.ubc.ca.

immunosuppressive action on T cells and macrophages. Involvement of $\alpha v\beta 6$ integrin-mediated activation of TGF-$\beta 1$ in the regulation of lung and skin inflammation has been demonstrated in $\beta 6$ integrin-deficient mice.[6] Double-knockout mice for $\beta 6$ integrin and TSP-1 have a more severe inflammatory phenotype that resembles that of TGF-$\beta 1$-null mice although in milder form.[23] Recent evidence indicates that integrin-mediated activation of TGF-$\beta 1$ plays a major role in immunoregulation *in vivo*. Mice with a nonfunctional variant of the RGD sequence (RGE) in LAP, the ligand for $\alpha v\beta 6$ integrin, cannot activate TGF-$\beta 1$ and, therefore, develop multiorgan mononuclear cell infiltrations.[24] Thus, it is likely that integrin-mediated activation of TGF-$\beta 1$ regulates inflammation in many tissues, including soft tissues of the oral cavity.

Periodontal diseases affect a large segment of the adult population leading to loss of teeth and also contributing to the total inflammatory burden associated with systemic conditions such as cardiovascular diseases.[25,26] Junctional epithelium (JE) plays a critical role in the adhesion of gingiva (gum) to tooth enamel and cementum, and this unique epithelium continuously renews itself by proliferating and migration along the tooth surface.[27,28] JE is also a critical tissue barrier, which, when breached by oral bacteria, initiates a robust, leukocyte-mediated immunological defense reaction within the gingival tissues. In periodontal disease, oral microbes and the host response induce JE to migrate apically and invade the gingival connective tissue during its transformation to pocket epithelium. Inflammation around the pocket epithelium then leads to the resorption of alveolar bone around the tooth, and thus also to the loss of the periodontal ligament attachment, which is normally responsible for suspending the tooth within the bone. The specific role of TGF-$\beta 1$ activation by $\alpha v\beta 6$ integrin or by other mechanisms in the maintenance or regulation of the immune defense in the gingiva is not known. It is known, however, that the periodontal disease process involves an imbalanced Th1/Th2 cytokine profile, resulting in high levels of interleukin-1β (IL-1β) and low levels of TGF-$\beta 1$.[29]

In the present study, we investigated the hypothesis that $\alpha v\beta 6$ integrin-mediated TGF-$\beta 1$ activation in the JE plays a major protective role in inflammatory periodontal disease. We report that $\alpha v\beta 6$ integrin is constitutively expressed in human and murine JE and that $\beta 6$ integrin-knockout mice develop all of the classic hallmarks of chronic periodontal disease. We further show in a rat model that initial signs of periodontal disease can be introduced by local blocking of $\alpha v\beta 6$ integrin-mediated TGF-$\beta 1$ activation. In addition, $\alpha v\beta 6$ integrin is strongly down-regulated in human periodontal disease, potentially by *Porphyromonas gingivalis*, the main pathogen for chronic periodontitis in humans.

Materials and Methods

Human Tissue Specimens

All of the procedures were approved by the Ethics Committee for Clinical Human Experimentation at the University of British Columbia. Twenty-one patients (15 males and 6 females; average age, 50 years) who presented with untreatable teeth requiring extraction for periodontal or other reasons and which could be feasibly extracted with gingival tissue attached were included in the present investigation. A total of 35 teeth were sampled. Both teeth with normal gingival apparatus (healthy controls) and teeth with periodontal involvement (deep pockets exceeding 5 mm and representing periodontal disease) were collected. A cohort of these patients were included in a wound healing study in which gingival tissue from periodontally involved teeth was excised from the tooth with a small blade, followed by curettage of the periodontal pocket using routine dental techniques. Tissue was then left to heal up to 28 days before the tooth with repairing tissue was extracted (minimum of two individuals per time point). Gingival tissue was removed from the tooth using a dental chisel and a dissecting microscope. Tissue samples were then placed in Tissue-Tek (OCT compound; Sakura Finetek USA, Inc., Torrance, CA) and snap-frozen in liquid nitrogen. Frozen sections (6 to 8 μm) were then cut using a cryostat and stored at -80°C until used for immunolocalization studies.

In one group of specimens, the tooth substance was carefully removed using a diamond bur, leaving only a thin layer of tooth with undisturbed soft tissue, including the JE, attached to it. The samples were then fixed with 4% formaldehyde in phosphate-buffered saline (PBS; pH 7.2) at room temperature for 2 hours. After this, the specimens were transferred into a decalcifying solution containing 12.5% ethylenediaminetetraacetic acid and 2% formaldehyde in distilled water and kept at $+4$°C. The solution was changed weekly for several weeks until the tooth was soft. When the decalcification was complete, the specimens were kept in 2.3 mol/L sucrose in PBS for 24 hours and then embedded in Tissue-Tek and frozen in liquid nitrogen. Cryostat sections (6 μm) were cut and stored at -80°C until used.

Animals

All animal procedures were approved by the Animal Care Committee of the University of British Columbia. The mice were maintained in a conventional animal care facility up to 12 months of age and allowed free access to standard mouse chow (Purina 5001; Purina, St. Louis, MO) and water. Homozygous integrin $\beta 6$-knockout mice (*Itgb6*$^{-/-}$; kindly provided by Dr. Dean Sheppard, University of California at San Francisco, San Francisco, CA)[6] were on a FVB background. Cohorts of 3-month-old mice (six mice in each group), 6-month-old mice (six mice in each group), and 12-month-old mice [14 *Itgb6*$^{-/-}$ and 18 wild-type (WT) mice] were studied. Animals were sacrificed by carbon dioxide inhalation. After decapitation, maxilla and mandible were separated and processed for analyses (see below). Male Sprague-Dawley rats (8 weeks old) were obtained from the Animal Care Centre of the University of British Columbia.

Assessment of Bone Loss

Mandibles were cut in half, and using a dissecting microscope, gingival tissue was removed and collected. The mandibles were then mechanically partially defleshed and exposed to 2% KOH until completely defleshed. To delineate the cemento-enamel junction (CEJ), dry mandibles were stained using Van Gieson's solution for 30 seconds followed by Ponceau S solution for 5 minutes. The stained jaws were then used for quantification of lingual alveolar bone loss as follows. Dried stained hemimandibles were placed under a dissecting microscope and aligned using dental impression putty so that the lingual and buccal cusps were superimposed. Using a digital camera (Eclipse TS100; Nikon, Tokyo, Japan), images, including the lingual view of first and second molars, were created from all of the jaws with the same measurement probe for calibration present in all images. Adobe Photoshop CS Me software (Adobe Systems, Inc., San Jose, CA) was used to standardize the images before any measurements. The area between the CEJ and the crest of the alveolar bone was quantified using ImageJ software (developed at the National Institutes of Health, Bethesda, MD, and available at *http://rsb.info.nih.gov/ij/*). The area of exposed root surface was documented for each tooth in pixel units as well as in mm^2. Repeated measurements on randomly selected teeth revealed an intraexaminer agreement of >98%.

To determine intrabony bone loss, high-resolution radiographs of hemi-mandibles (six in each group) were captured with the Faxitron MX-20 radiography system (Faxitron X-Ray Corporation, Wheeling, IL). Intrabony bone loss around the first and second molars was analyzed using a visual scale of 0 to 3 (0, no bone loss; 1, horizontal and vertical bone loss less than one third of the root length; 2, horizontal or vertical bone between one and two thirds of the root length; 3, horizontal or vertical bone loss more than two thirds of the root length). Furthermore, the bone loss between the teeth and individual roots after the crowns of teeth were removed with a fine bur was visualized by scanning electron microscopy using routine methods.

Rat Model of Gingival Inflammation

The rats were randomly divided into four groups (six mice in each group) before treatment. All rats were anesthetized with isoflurane (^{Pr}AErrane; Baxter Corporation, Mississauga, Canada), placed on their backs and kept under anesthesia, while their mouths were kept open with an orthodontic stainless steel wire piece. The first group was treated with 3×0.3 μl of lipopolysaccharide (LPS) (*Escherichia coli*, 25 μg/μl in pyrogen-free water; Sigma BioSciences, St. Louis, MO), the second with a combination of LPS and 6.3G9 monoclonal antibody (50 μg/ml, a potent inhibitor of αvβ6-mediated TGF-β1 activation; kindly provided by Drs. Shelia M. Violette and Paul H. Weinreb, Biogen Idec, Inc., Cambridge, MA),[30] the third with a combination of LPS and 7.8B3 monoclonal antibody (50 μg/ml; a nonblocker of β6 integrin),[30] and the fourth group with pyrogen-free water only. The antibodies used for the study have been extensively tested for specificity and effectiveness.[30] Briefly, the IC_{50} for blocking αvβ6 integrin binding to LAP is 2.7 ng/ml for 6.3G9 (blocking antibody) and >10,000 ng/ml for 7.8B3 (control antibody). The IC_{50} for blocking TGF-β activation via αvβ6 integrin is 0.5 ng/ml for 6.3G9 whereas 7.8B3 does not block activation. The antibodies and LPS were administered with a micropipette directly into the palatal gingiva of the two molar teeth on both sides of the maxilla. Each group was treated at the same time of the day until the end of the experiment. After 8 weeks, all animals were euthanized, and the maxilla was dissected for histology.

Histology

The maxillae of the FVB and β6 integrin-knockout mice were decalcified in PBS containing 0.4 mol/L ethylenediaminetetraacetic acid and 2% formaldehyde. The solution was changed every other day for 6 weeks. The rat mandibles and maxillae were treated similarly. The specimens were then processed for embedding in paraffin and sectioning using routine protocols. The specimens were sectioned (7 μm) in the bucco-lingual or mesio-distal direction. Every 10th slide from each block of sections was stained with hematoxylin and eosin (H&E). Stained sections were used to assess the migration of JE and the level of inflammation by light microscopy. Using a digital camera, images were captured from all stained sections with a standard scale and transferred to Adobe Photoshop CS Me. The migration of epithelial tissue (junctional or pocket epithelium) was measured in mm or in pixels using the ImageJ program. Inflammation underneath the epithelial tissue was scored using a visual scale of 0 to 3 (0, no inflammatory cells present; 1, scattered mild inflammatory infiltrate; 2, moderate inflammatory infiltrate; 3, heavy inflammatory infiltrate). In the rat model, the inflammatory infiltrate adjacent to the epithelium was quantified in H&E-stained sections using a combination index based on both the area occupied by inflammatory cells and the inflammatory cell density. Briefly, 15 tissue sections for three individual rats in a group were analyzed using a light microscope with a microscopic grid of 100 squares in 1 mm^2 (Axiolab E; Zeiss, North York, Canada) and ×20 magnification. The area occupied by inflammatory cells was determined by counting the squares in the grid containing the inflammatory infiltrate immediately adjacent to the epithelium. An index of 1 to 5 was assigned to this measurement. The density of infiltrate was determined by counting the number of leukocytes found in 10 randomly selected squares. Again, each measurement was scored from 1 to 5 (1, 0 to 9 cells per field; 2, 10 to 19 cells per field, and so forth). To determine the final histological inflammation index, the two measurements were added together. In addition to H&E staining, a cohort of slides in each experiment was stained with Movat pentachrome for qualitative assessment of cellular and extracellular matrix components.

Immunohistochemistry

Primary antibodies used for immunostaining were: cytokeratin 19 (CK19; sc-6278; Santa Cruz Biotechnology, Inc., Santa Cruz, CA), laminin-5 (ab1207; Abcam, Inc., Cambridge, MA), tenascin-C (T-2551, Sigma), EDA-fibronectin (OBT0082; Accurate Chemical and Scientific, Westbury, NY), TGF-β1 (sc-7892, Santa Cruz Biotechnology) and αvβ6 integrin (β6B1, kindly provided by Dr. Dean Sheppard; recognizes both human and mouse).[31]

Frozen sections were fixed with acetone (−20°C) for 5 minutes, rinsed, and incubated in normal blocking serum (Vectastain; Vector Laboratories, Inc., Burlingame, CA) in a humidified chamber at room temperature for 30 minutes. After rinsing, the sections were incubated overnight with the primary antibody of interest, which was diluted in PBS containing bovine serum albumin (1 mg/ml, Sigma) and 0.01% Triton X-100. They were then rinsed and incubated with a biotinylated, fluorescein isothiocyanate- or Alexa Fluor 488-conjugated secondary antibody (Invitrogen Detection Technologies, Eugene, OR) for 1 hour. In the samples incubated with biotinylated antibodies, the reaction was followed by incubation with ABC avidin/peroxidase reagent (Vectastain Elite Kit, Vector Laboratories). The sections were then rinsed and reacted with Vector VIP substrate peroxidase for the appropriate time for each antibody. To stop the reaction, the sections were rinsed with distilled water for 10 minutes. They were then allowed to air dry, mounted using Vectamount permanent mounting medium (Vector Laboratories), viewed, and photographed using a light microscope. For nuclear staining, the sections were stained for 5 minutes with 0.5 μg/ml of 4,6-diamidino-2-phenylindole (Sigma) in the dark and then rinsed with PBS. Fluorescently labeled specimens were rinsed and mounted using Immu-Mount medium (Thermo Shandon, Pittsburgh, PA) and viewed using a fluorescence microscope (Axioplan2, Zeiss). Images were captured using a QIcam camera (Burnaby, Canada) mounted to the microscope and fed directly to the Northern Eclipse software program (Haverhill, Suffolk, UK).

Analysis of MMP Expression in Mouse Gingiva by Gelatin Zymography

The gingiva around molar teeth was excised from six *Itgb6*$^{-/-}$ and six WT mice. Each sample was ground over dry ice using a mortar and pestle. One ml of cold Dulbecco's modified Eagle's medium (Gibco, Invitrogen Corporation, Grand Island, NY) containing 0.1% pyrogen-free bovine serum albumin and 1× Complete protease inhibitor cocktail (Roche Applied Science, Laval, Canada) was added to each 20 mg of homogenized tissue. The suspended tissues were sonicated three times for 10 seconds on ice. Tissue debris was removed from the samples by centrifugation (10,000 rpm for 10 minutes at +4°C), and filtering through a 0.2-μm syringe filter. Twenty-five μl of each sample was then separated in a 4%/10% sodium dodecyl sulfate-polyacrylamide gel electrophoresis gel containing 1 mg/ml of fluorescently labeled gelatin as a substrate for gelatinases. The gelatin zymography gels were developed as described previously.[32] The gels were illuminated with UV light, and the images were captured with a digital camera. The band intensities were quantified using the ImageJ software.

Bacteria and LPS Preparations

P. gingivalis (ATCC 33277), *Treponema denticola* (ATCC 35405), *Fusobacterium nucleatum* subsp. *nucleatum* (ATCC 25586), and *Tannerella forsythensis* (ATCC 43037) were grown in their appropriate culture media.[33] LPS were isolated from these bacterial strains as previously reported,[34] using proteinase K digestion of a whole cell extract and successive solubilization and precipitation steps. The LPS preparations were freeze-dried and kept at −20°C. The amount of contaminating protein was evaluated using a protein assay kit (Bio-Rad Laboratories, Mississauga, Canada) with bovine serum albumin as a control, and it was less than 0.001% in all LPS preparations. A whole cell extract of *P. gingivalis* was prepared as follows. Freeze-dried bacteria were suspended in distilled water and sonicated at 200 W with pulse mode on ice for 10 × 30 seconds. Unbroken cells and large membrane fragments were removed by centrifugation (10,000 × *g* for 15 minutes). The cell lysate was freeze-dried and kept at −20°C.

Cell Culture, Real-Time PCR, and Flow Cytometry

The spontaneously immortalized gingival keratinocytes[35] were maintained in Dulbecco's modified Eagle's medium supplemented with 23 mmol/L sodium bicarbonate, 20 mmol/L HEPES, antibiotics (50 μg/ml streptomycin sulfate, 100 U/ml penicillin) and 10% heat-inactivated fetal bovine serum (Gibco). To investigate the regulation of β6 integrin expression in keratinocytes, the cells (6×10^5) were seeded into six-well plates in Dulbecco's modified Eagle's medium, which were precoated with 10 μg/ml of type I collagen in 0.012 mol/L HCl at +4°C overnight followed by washings and blocking with 1% heat-denatured bovine serum albumin for 48 hours. The cells were allowed to attach for 2 hours and then treated with TGF-β1 (10 ng/ml; Chemicon International, Temecula, CA), IL-1β (500 ng/ml; Sigma), prostaglandin E2 (200 ng/ml; Sigma), tumor necrosis factor-α (TNF-α) (200 ng/ml; Chemicon), IL-6 (100 ng/ml, Chemicon), LAP (1 μg/ml; Sigma), a function-blocking anti-TGF-β1,2,3 antibody (10 μg/ml; R&D Systems, Inc., Cedarlane Laboratories Ltd., Burlington, Canada), or PBS only as a control for 24 hours. In a set of experiments, the cells were treated with a whole cell extract of *P. gingivalis* (10 μg/ml) or the LPS fractions (50 μg/ml) of *P. gingivalis*, *T. denticola*, *F. nucleatum*, *or T. forsythensis.* The treatments were repeated two to seven times. In some experiments, the *P. gingivalis* extract was heated for 10 minutes at 100°C before cell treatment. Total RNA was extracted from the treated keratinocytes using the NucleoSpin RNA II kit (Macherey-Nagel Inc., Bethlehem, PA) and treated with DNase I

digestion. Total RNA integrity was verified by agarose gel electrophoresis, and total RNA concentration was measured by spectrophotometry at 260 nm. Total RNA (1 μg) was reverse-transcribed with oligo(dT) primers using iScript Select cDNA synthesis kit (Bio-Rad Laboratories, Hercules, CA) according to the manufacturer's instructions. Each RT product was diluted to a concentration with a threshold-cycle value well within the range of its standard curve. Amplification reactions were conducted for β6 integrin with β-actin as a reference in triplicates. Five μl of each diluted RT product was mixed with 10 μl of 2× iQ SYBR Green I Supermix (Bio-Rad) and either 15 pmol of β-actin primers or 10 pmol of β6 integrin primers in a final volume of 20 μl. The primers for β-actin were 5′-CTGTGGCATCCACGAAAC-3′ and 5′-CAGACAGCACTGTGTTGG-3′, corresponding to nucleotides 886 to 903 and 957 to 974 of β-actin cDNA, respectively. The primers for β6 integrin were 5′-CGCTGTAACCCAAGAACAAG-3′ and 5′-TGTTTCCGGAGTCCTTCTGA-3′, and they were designed to produce a 95-bp cDNA fragment. Real-time PCR amplification was performed with the MiniOpticon real-time system (Bio-Rad) (program: 3 minutes at 95°C, followed by 40 cycles of 15 seconds at 94°C, 20 seconds at 58°C, 20 seconds at 72°C). The data were analyzed with Gene Expression Analysis for iCycler iQ Real-Time PCR detection system software (Bio-Rad).

The effect of *P. gingivalis* on the cell surface expression of αvβ6 integrin in gingival keratinocytes was analyzed by flow cytometry as described previously.[36] Briefly, 6×10^5 cells were seeded into six-well plates in their complete growth medium for 24 hours. The cells were then washed with PBS and exposed to 10 ng/ml of TGF-β1, 10 ng/ml of TGF-β1 plus 40 μg/ml of freeze-dried cell lysate of *P. gingivalis*, or the bacterial cell lysate alone in Dulbecco's modified Eagle's medium for 18 hours. The cells were detached and reacted with monoclonal antibody against human αvβ6 integrin (MAB2077, Chemicon) followed by donkey anti-mouse Alexa Fluor 488-conjugated IgG (Invitrogen) and washes. The samples were analyzed with FACSCalibur flow cytometer (BD Biosciences, Mississauga, Canada).

Statistical Analysis

The Student's *t*-test was used to determine whether the differences in MMP expression in WT and *Itgb6*$^{-/-}$ mice were statistically significant. Comparison of parametric data between WT and *Itgb6*$^{-/-}$ mice, including the differences in alveolar bone loss and the migration of the epithelial tissue were also achieved with the Student's *t*-test. The nonparametric data, including severity of inflammation and degree of bone loss from radiographical images, were analyzed using the Mann-Whitney *U*-test. One-way analysis of variance and Tukey's posttest were used to analyze the differences in β6 integrin expression in gingival keratinocytes as well as for the analyses of rat JE migration. The statistical significance was set at $P < 0.05$.

Results

The αvβ6 Integrin Is Constitutively Expressed in the Epithelium of Human and Murine Gingiva that Interfaces with Enamel (JE) and Co-Localizes with TGF-β1

We have previously shown that oral epithelium and epidermis lack αvβ6 integrin expression but that it is induced in wound epithelium during tissue repair.[3] The specialized epithelium (JE) that links gingiva to the tooth enamel mimics wound epithelium in many respects. Therefore, we investigated whether αvβ6 integrin is expressed in the JE of fully erupted teeth by immunohistochemistry. In human gingival soft tissue specimens, the JE was identified by morphology and also with antibodies against specific molecular markers—cytokeratin 19 (CK19) and laminin-5.[28] As expected, CK19 was highly expressed in the JE cells between the gingival connective tissue and enamel (Figure 1A). Laminin-5 decorated both the external basal lamina against the connective tissue and internal basal lamina against the tooth (Figure 1A). All epithelial keratinocytes in the JE strongly expressed αvβ6 integrin (Figure 1A). We then localized the expression of some of the known ligands of αvβ6 integrin in these specimens. Tenascin-C was localized mainly at the basement membrane zone against the connective tissue whereas EDA-fibronectin was localized throughout the connective tissue stroma (Figure 1A). Expression of TGF-β1, however, was localized in all cell layers of the JE, thus co-localizing in the same area as αvβ6 integrin (Figure 1A). The most apical epithelial tissue attached to the tooth is often lost when removing the soft tissue from the tooth. Therefore, to further confirm these observations, we prepared frozen sections of decalcified teeth that were removed with small amounts of gingival soft tissue present. The narrow JE present in these specimens between the enamel and the connective tissue was positive for the specific markers (CK19 and laminin-5) and for αvβ6 integrin (data not shown). To determine whether αvβ6 integrin is also expressed in rodent JE, we immunostained frozen sections of both rat and mouse JE with specific antibodies recognizing murine epitopes of αvβ6 integrin. In agreement with the human specimens, αvβ6 integrin was expressed in all cell layers of the murine and rat JE (Figure 1B).

During Repair of the JE, the Expression of αvβ6 Integrin Is Rapidly Restored

Gingival tissue is prone to regular trauma from mastication and from routine use of oral hygiene aids (such as tooth brushing). To investigate whether the expression of αvβ6 integrin is restored after repair of gingival tissue after surgical trauma, we removed the soft tissue adjacent to teeth in volunteers and followed healing of the tooth-soft tissue interface for up to 28 days. Specimens collected immediately

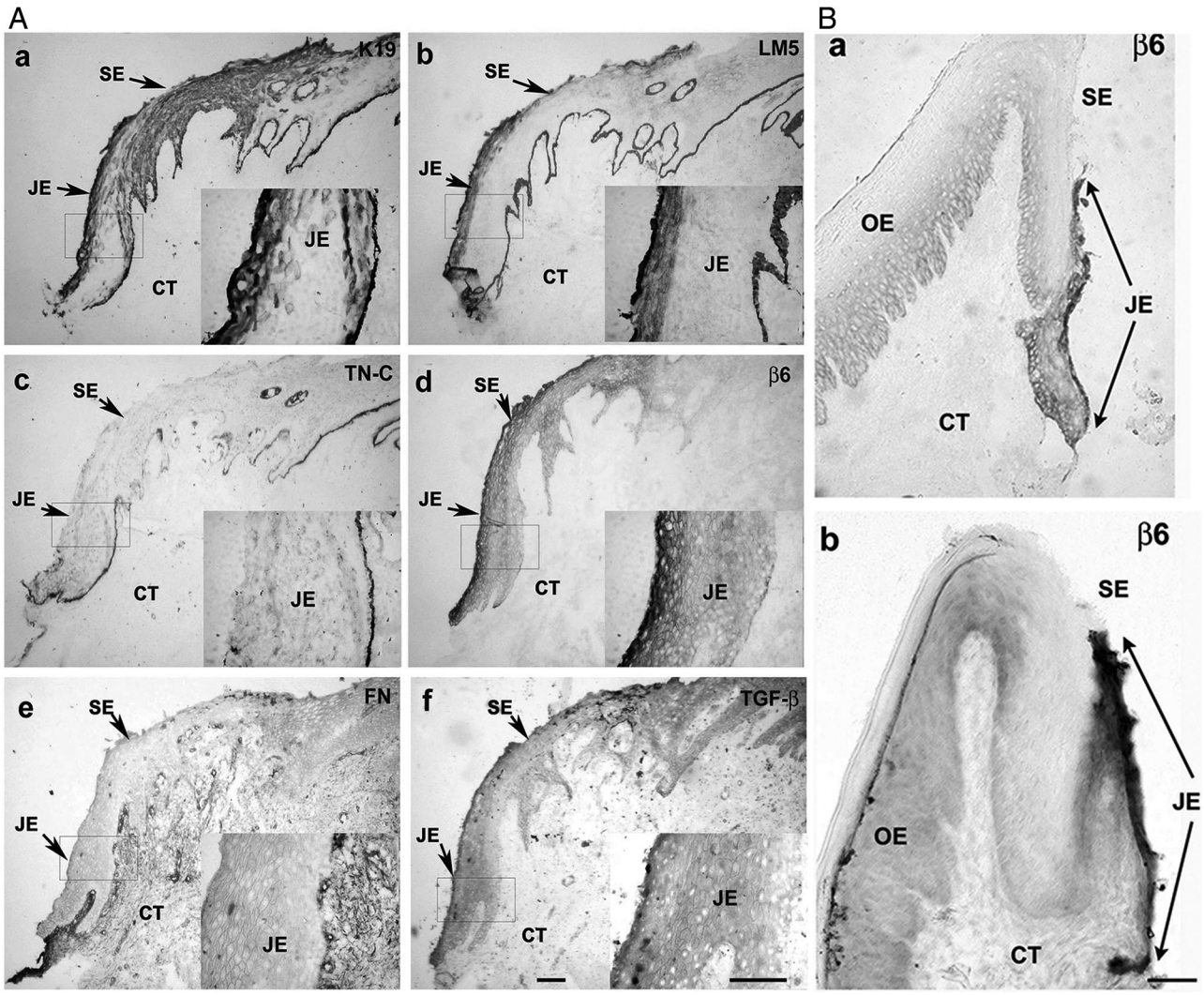

Figure 1. JE expresses $\alpha v\beta 6$ integrin and TGF-$\beta 1$. **A:** Immunolocalization of CK19 (**a**), laminin-5 (**b**), tenascin-C (**c**), $\alpha v\beta 6$ integrin (**d**), EDA-fibronectin (**e**), and TGF-$\beta 1$ (**f**) in JE from fully erupted human teeth. **B:** Immunolocalization of $\alpha v\beta 6$ integrin in rat (**a**) and mouse (**b**) gingiva from molar teeth. **Insets** show magnified area indicated by a box in each panel. CT, connective tissue; SE, sulcular epithelium; OE, oral epithelium. Scale bars = 100 μm.

after tissue removal without any healing time showed efficient removal of the JE (Figure 2). In 1-day-old wounds, the epithelial edge showed initial signs of migration into the fibrin clot (Figure 2). This migration continued in 3-day-old wounds and reached the most apical detectable level after 7 days (Figure 2). Immunolocalization of CK19 showed that some CK19-positive keratinocytes remained next to the initial wound immediately after wounding (Figure 2). During the migratory phase, only the CK19-positive cells moved into the wound provisional matrix of the wound (Figure 2). In 7-day-old wounds, all cells in the JE expressed CK19 (Figure 2). Integrin $\alpha v\beta 6$ was strongly expressed in the JE of nonwounded specimens, but was absent from the soft tissue immediately after wounding (Figure 2). Cells advancing to the wound bed in 1-day-old wounds expressed low levels of $\alpha v\beta 6$ integrin (Figure 2). However, after 3 days of healing, the migrating cells became strongly positive for $\alpha v\beta 6$ integrin and its expression remained unchanged during later time points of the study (Figure 2). Expression of EDA-fibronectin was limited to the connective tissue, and tenascin-C was expressed strongly at the basement membrane zone of JE and the blood vessels (data not shown). Tenascin-C was also occasionally observed at the soft tissue-tooth interface (data not shown).

Expression of $\alpha v\beta 6$ Integrin Is Strongly Down-Regulated in Periodontal Disease

In periodontal disease, JE transforms to an invasive pocket epithelium, which shows unique pathological features such as ulcerations and formation of epithelial ridges that are surrounded by a heavy inflammatory infiltrate. To investigate the expression of $\alpha v\beta 6$ integrin in the invasive pocket epithelium, we collected specimens of periodontally diseased tissue from a number of individuals with deep periodontal pockets around their teeth. Expression of $\alpha v\beta 6$ integrin in four such patients is demonstrated in Figure 3. All specimens

showed epithelial invasion into heavily inflamed connective tissue (Figure 3). Compared to normal JE, the expression of CK19 was reduced in pocket epithelium of some specimens (Figure 3, patients 1 and 2). Expression of αvβ6 integrin was strongly down-regulated in all specimens (Figure 3), even in those that had maintained CK19 expression.

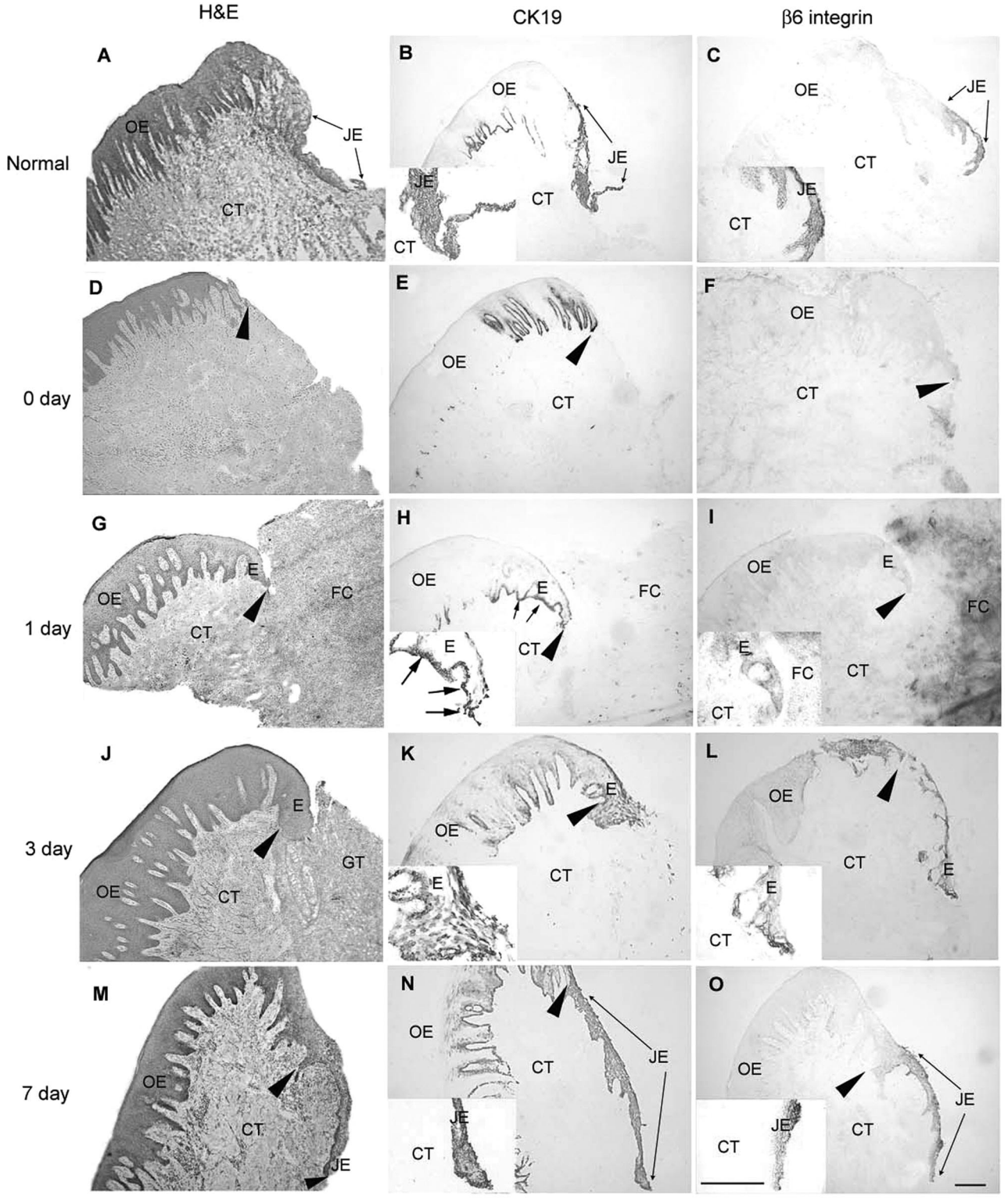

Figure 2. The expression of αvβ6 integrin is restored in healing JE. JE was removed surgically, and samples of the healing tissue were collected immediately after tissue removal (**D–F**) and after 1 (**G–I**), 3 (**J–L**), or 7 (**M–O**) days of healing. Normal tissue (**A–C**) is shown as a control. H&E staining of healing tissue (**A**, **D**, **G**, **J**, **M**); immunolocalization of CK19 (**B**, **E**, **H**, **K**, **N**) and αvβ6 integrin (**C**, **F**, **I**, **L**, **O**). **Arrowheads** point to the wound edge. Higher magnifications of the migrating epithelial front and restored JE are shown in the **insets**. CT, connective tissue; GT, granulation tissue; OE, oral epithelium; E, epithelium; FC, fibrin clot. Scale bar = 200 μm.

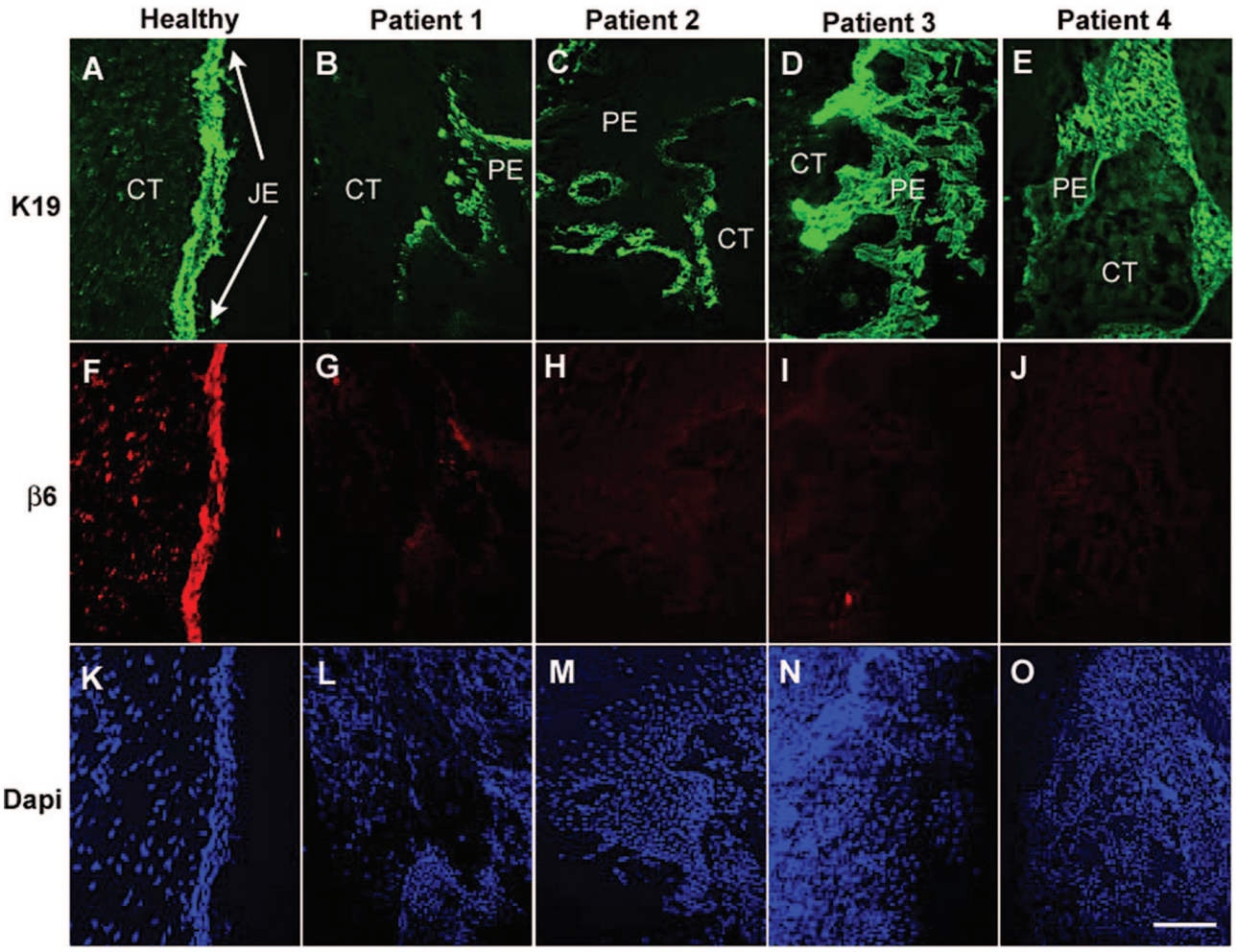

Figure 3. The expression of integrin $\alpha v\beta 6$ is down-regulated in periodontal disease. Tissue was collected from four patients. Healthy tissue was collected as a control. Tissue sections from individuals with periodontal disease (**B–E**, **G–J**, **L–O**) or from healthy patients (**A**, **F**, **K**) were immunostained for CK19 (**A–E**) and $\alpha v\beta 6$ integrin (**F–J**). 4,6-diamidino-2-phenylindole staining (**K–O**) was performed to highlight the nuclei. CT, connective tissue; PE, pocket epithelium. Scale bar = 200 μm.

Expression of $\alpha v\beta 6$ Integrin Is Reduced in Gingival Keratinocytes by P. gingivalis

Having established that $\alpha v\beta 6$ integrin is constitutively expressed in JE of healthy gingiva but strongly down-regulated in periodontal disease, we investigated whether cytokines and bacterial products could be responsible for the reduced expression levels. A number of cytokines (prostaglandin E2, TNF-α, IL-1β, IL-6) and LPS from pathogens (*P. gingivalis*, *T. denticola*, *F. nucleatum*, *T. forsythensis*)[37] involved in the pathogenesis of periodontal disease were tested for regulation of $\beta 6$ integrin mRNA expression in human gingival keratinocytes under various culture conditions and concentrations. Only negligible effects were observed (Figure 4A, and data not shown). As reported previously for other epithelial cell lines, TGF-$\beta 1$ strongly increased the expression of $\beta 6$ integrin mRNA and $\alpha v\beta 6$ integrin cell surface levels in gingival keratinocytes (Figure 4, A and B). When whole extract of the chronic periodontal disease-associated pathogenic bacterium, *P. gingivalis*, was added simultaneously with TGF-$\beta 1$, it effectively prevented the stimulation of $\alpha v\beta 6$ integrin expression by TGF-$\beta 1$ (Figure 4B). The active component in the bacterial extract was found to be heat-labile, because heating the extract (10 minutes, 100°C) abolished the inhibitory effect (data not shown). Blocking endogenous TGF-$\beta 1$ signaling with LAP or anti-TGF-$\beta 1$ antibody reduced the expression of $\beta 6$ integrin mRNA in keratinocytes by ~50% (Figure 4C), suggesting that endogenous TGF-$\beta 1$ plays a major role in the regulation of the basal expression level of $\alpha v\beta 6$ integrin.

Mice Deficient in $\alpha v\beta 6$ Integrin Show Hallmarks of Human Periodontal Disease

To investigate whether the lack of $\alpha v\beta 6$ integrin is directly involved in the initiation of periodontal disease, we first assessed whether $\beta 6$ integrin-knockout mice (*Itgb6*$^{-/-}$) have any abnormalities in the development or maintenance of soft tissue attachment to their molar teeth. In the first cohort of 6-month-old mice, we observed striking alterations in the organization of JE in the *Itgb6*$^{-/-}$ mice. There were no obvious changes, however, in overall

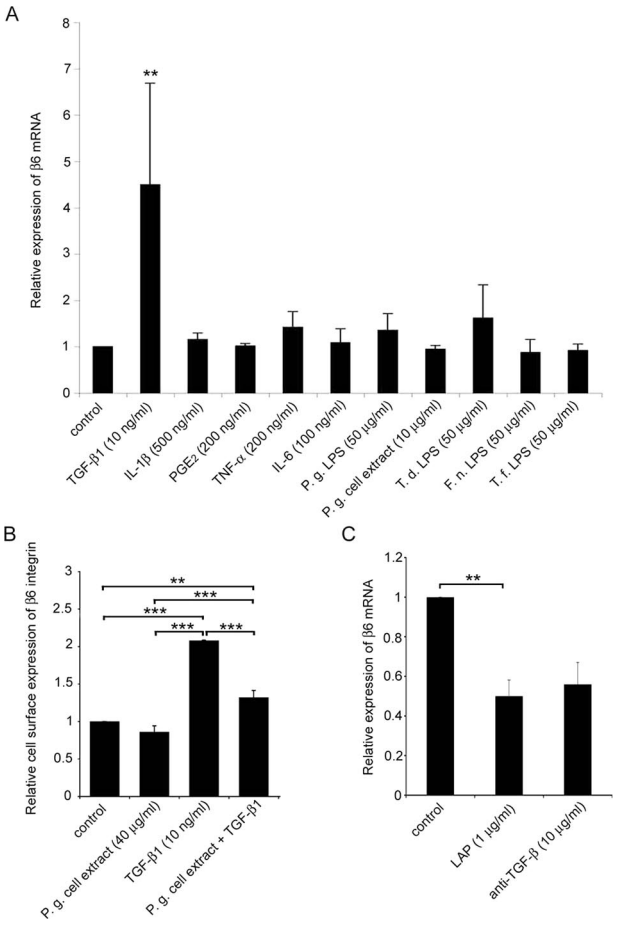

Figure 4. *P. gingivalis*, LAP, and anti-TGF-β1 reduce $\alpha v\beta 6$ integrin expression in cultured gingival keratinocytes. **A:** Gingival keratinocytes were treated with cytokines (TGF-β1, IL-1β, prostaglandin E2, TNF-α, IL-6), bacterial LPS (*P. gingivalis*, *T. denticola*, *F. nucleatum*, *T. forsythensis*), or *P. gingivalis* whole cell lysate. Total RNA was extracted, and the expression of β6 integrin subunit was analyzed by real-time PCR using β-actin as a control. PCR reactions were performed in triplicates, and the experiments were repeated four to seven times. **B:** The cells were exposed to cell lysate of *P. gingivalis*, TGF-β1, or a combination of both. Total cell surface expression of $\alpha v\beta 6$ integrin was measured by flow cytometry. The experiment was repeated three times. **C:** The cells were treated with LAP or function-blocking anti-TGF-β1 antibody. Relative expression of β6 integrin was analyzed as in **A**. The experiment was repeated three times. Relative β6 integrin expression is expressed as mean ± SD of parallel experiments in all figures. Only differences that were deemed statistically significant are indicated: $^{*}P < 0.05$; $^{**}P < 0.01$, $^{***}P < 0.001$ (analysis of variance and Tukey's post test or Student's *t*-test). Results of the effect of anti-TGF-β1 antibody treatment are from a single experiment, and SD was calculated from three parallel samples.

structure of the molars or their eruption rate in these animals. In WT mice, the epithelium showed typical features of normal murine JE, which extends down and then reflects back up against the enamel surface, with most apical cells being near the CEJ (Figure 5A). Interestingly, the JE of *Itgb6*$^{-/-}$ mice showed disorganization, invasion into the connective tissue, migration along the root surface, and inflammatory infiltrate around the epithelial tissue (Figure 5A). However, there was no evidence for separation of the epithelium from the tooth, suggesting that that the physical adhesion of JE to the tooth was not altered. To investigate further the progression of the histopathological changes of the tooth attachment apparatus in *Itgb6*$^{-/-}$ mice, we subjected a group of 12-month-old mice to qualitative assessment of cellular and extracellular matrix components using histological staining. In the aged WT mice, the JE continued to demonstrate normal structure and its adhesion remained close to the CEJ (Figure 5B). In *Itgb6*$^{-/-}$ mice, however, the JE had transformed to a typical pocket epithelium extending in some specimens to more than 50% of the root length (Figure 5B). In addition, epithelial invasions were seen inside the connective tissue, forming abscess-like lesions full of mononuclear inflammatory cells (Figure 5B). We then quantified the distance of epithelial migration in stained paraffin sections of multiple teeth from six 12-month-old mice. WT mice showed minimal migration of JE beyond the CEJ. In contrast, the JE of *Itgb6*$^{-/-}$ mice showed significantly ($P < 0.01$) more migration with an average of ~0.4 mm (Figure 6A).

To verify whether apical migration of JE was associated with chronic inflammation, we quantified the relative number of inflammatory cells adjacent to the JE in WT mice and *Itgb6*$^{-/-}$ mice. The results showed a significantly higher inflammatory score for sites in *Itgb6*$^{-/-}$ mice with epithelial migration compared to those in the WT mice with negligible migration (Figure 6B), indicating that formation of pocket epithelium was associated with inflammation.

Expression of high levels of MMPs is associated with inflammatory periodontal disease.[38] Therefore, we analyzed the amount of gelatin-degrading MMPs in the gingival extracts from four 12-month-old WT and five *Itgb6*$^{-/-}$ mice by zymography. In WT mice, proMMP-9 and proMMP-2, with small amounts of active MMP-2 and MMP-9 were present (Figure 6C). In *Itgb6*$^{-/-}$ mice, the expression of active MMP-2 and MMP-9 was increased (Figure 6, C and D). In addition, four of these samples contained elevated amounts of unknown, low molecular weight gelatinases (Figure 6, C and D).

Taken together, we have now demonstrated at the histopathological and biochemical level that *Itgb6*$^{-/-}$ mice possess two of the three hallmarks of spontaneous periodontal disease: formation of periodontal pockets and inflammation. To investigate whether they also suffered from alveolar bone loss around the molar teeth (the third hallmark of periodontal disease), a number of assays were performed. The histological analysis of a limited number of specimens had shown that the level of tooth-supporting alveolar bone was reduced and that active bone resorption with multinucleated osteoclasts was present in many specimens (Figure 5B). To quantify the bone loss at the lingual surfaces of the molars, the jaws from both genders were defleshed and stained to measure the area of exposed root surface (Figure 7A). The WT mice showed some exposed root surface at the age of 3 months, which represents the normal distance between alveolar crest and CEJ (the so-called "biological width"). This distance did not change until the mice aged to 12 months, at which point there was some exposure of the root surfaces present (Figure 7, A and B). There was, however, a significantly larger area of root exposure in the *Itgb6*$^{-/-}$ mice compared to WT mice in all age groups, indicating that bone loss in these animals started early and progressed with age (Figure 7, A and B). In the *Itgb6*$^{-/-}$ group, several mice showed severe bone loss

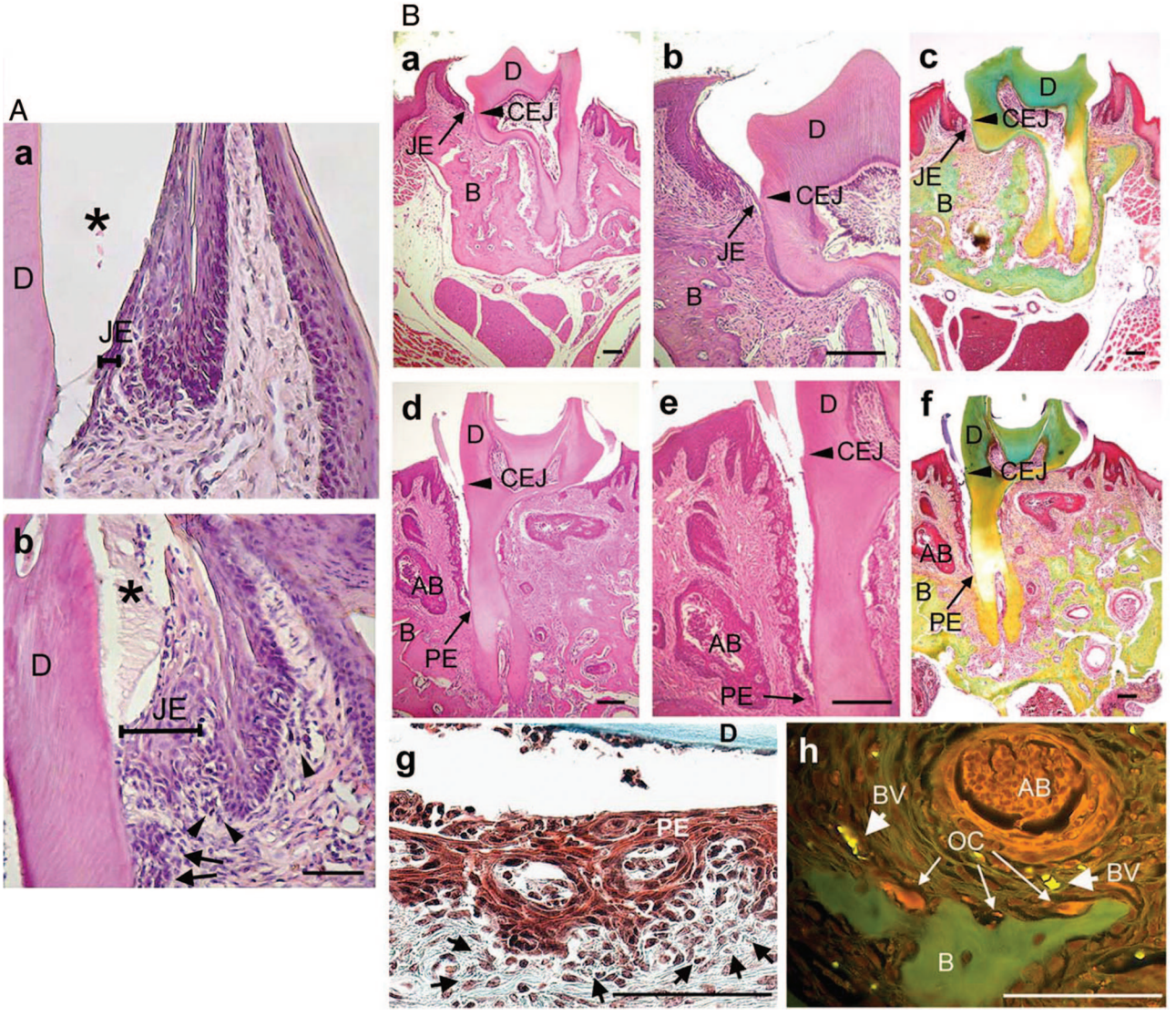

Figure 5. The JE of β6 integrin knockout mice shows epithelial invasion into the connective tissue, migration along the root surface, and increased inflammation. **A:** H&E staining of the JE of 6-month-old WT (**a**) and *Itgb6*$^{-/-}$ mice (β6$^{-/-}$, **b**). D, dentin; **asterisk**, enamel. **Arrows** point to invading epithelial cells, and **arrowheads** mark infiltrated inflammatory cells. **B:** H&E staining (**a**, **b**, **d**, **e**) and pentachrome staining (**c**, **f**) of the JE of 12-month-old WT (**a–c**) and *Itgb6*$^{-/-}$ mice (**d–f**). Green color in the Movat pentachrome-stained tissues indicates collagen. **g** and **h:** Enlarged image of the H&E-stained pocket epithelium and the pentachrome staining of a bone lesion in the *Itgb6*$^{-/-}$ mice, respectively. **Small arrows** in **g** point to infiltrated inflammatory cells. PE, pocket epithelium; D, dentin; B, alveolar bone; AB, abscess-like lesion surrounded by epithelial cells; BV, blood vessel; OC, osteoclast. Scale bars = 100 μm.

extending between the roots of molar teeth, and three teeth (5%) were actually lost because of advanced bone loss (Figure 7C). There was no gender preference for the bone loss (data not shown). Because periodontal disease typically starts and progresses faster between the teeth, creating intrabony defects that can remain hidden when exposed root surfaces are examined from the lingual or buccal surfaces, we produced high-resolution radiographs to assess the intrabony bone loss. In an additional cohort of animals, we also removed the crowns of teeth to allow for a better view of intraosseous defects and tooth relationships by scanning electron microscopy. Both the radiographs and the scanning electron microscopy revealed extensive bone resorption between the roots of the teeth in the *Itgb6*$^{-/-}$ mice whereas no such defects were found in the WT mice (Figure 8A). We then quantified the bone loss in the radiographs using a bone-loss index. The results showed significantly more bone loss in the *Itgb6*$^{-/-}$ compared to the WT mice (Figure 8B), indicating that bone loss in *Itgb6*$^{-/-}$ mice followed a similar pattern to that seen in human periodontal disease.

Antibody Blocking of αVβ6 Integrin-Mediated Activation of TGF-β1 Induces Epithelial Migration and Inflammation in a Rat Model of Periodontal Disease Initiation

To investigate whether the changes observed in *Itgb6*$^{-/-}$ mice were caused by altered TGF-β1 signaling, we used a rat model,[39,40] in which the early signs of periodontal

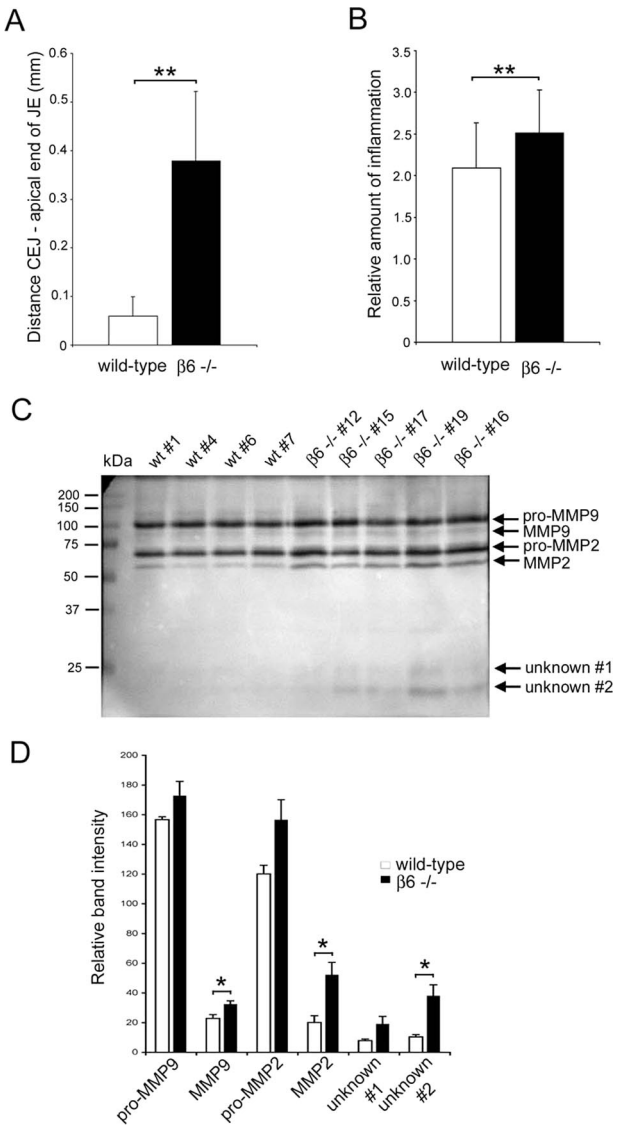

Figure 6. Twelve-month-old β6-knockout mice show significantly increased epithelial migration, higher levels of inflammation, and elevated expression of active MMPs. **A:** Quantitative assessment of the distance of epithelial migration in stained paraffin sections representing multiple teeth from WT ($n = 6$) and *Itgb6*$^{-/-}$ mice ($\beta6^{-/-}$, $n = 6$). **B:** The relative number of inflammatory cells adjacent to the JE in WT ($n = 6$) and *Itgb6*$^{-/-}$ mice ($n = 6$) with apical migration. **C:** MMPs in the gingival extracts from WT ($n = 4$) and *Itgb6*$^{-/-}$ mice ($n = 5$) were analyzed by gelatin zymography. The quantified band intensities are shown in **D**. Results are expressed as mean ± SD in all figures. Only differences that were deemed statistically significant are indicated: $^{*}P < 0.05$; $^{**}P < 0.01$ (Student's *t*-test or Mann-Whitney *U*-test).

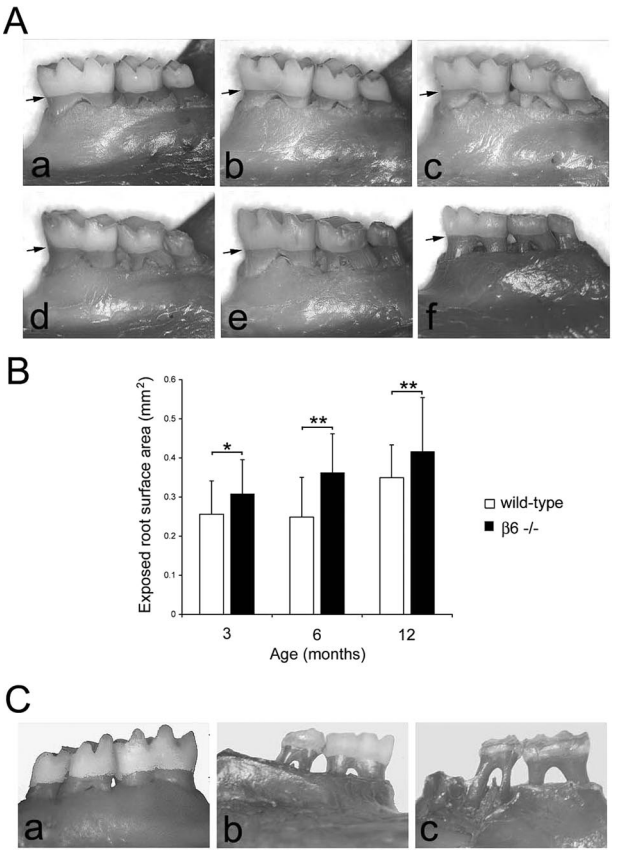

Figure 7. β6 integrin-knockout mice develop severe alveolar bone loss. **A:** The jaws of 3-month-old (**a**, **d**), 6-month-old (**b**, **e**), and 12-month-old (**c**, **f**) WT (**a–c**) and *Itgb6*$^{-/-}$ mice ($\beta6^{-/-}$, **d–f**) were defleshed and stained to show the area of exposed root surface. **Arrows** mark the CEJ. **B:** The exposed area between the CEJ and the crest of the alveolar bone of the first and second molars was quantified. Mean values of 48 teeth from 3- and 6-month-old mice and 125 teeth from 12-month-old mice ± SD are presented. Statistically significant differences are indicated: $^{*}P < 0.05$; $^{**}P < 0.01$ (Student's *t*-test). **C:** Examples of severe bone loss extending between the roots of molar teeth in 12-month-old *Itgb6*$^{-/-}$ mice (**c**, **d**). The jaw of a WT mouse is shown in **a** for comparison.

disease can be initiated in a relatively short period of time, to block the αvβ6 integrin-mediated TGF-β1 activation by a specific antibody. Ligatures have been extensively used for creation of periodontal defects, mainly for studies aimed at therapeutical interventions.[41] We choose not to use the ligature model because the insertion of ligature would cause trauma at the base of the gingival sulcus and would potentially confuse the results, keeping in mind that expression of αvβ6 integrin is induced in wound healing.[3] Control rats treated by daily application of water for 8 weeks at the gingival crevice showed no changes in the structure or position of the JE (Figure 9, A and B), whereas those that were exposed to LPS showed some apical migration of the JE. Animals treated with LPS and a nonfunction-blocking αvβ6 integrin antibody (7.8B3), also showed some apical migration of the JE. A combination of LPS and 6.3G9 antibody, which potently blocks αvβ6 integrin-mediated TGF-β1 activation,[30] significantly increased the apical migration of JE along the root surface compared to other treatments, thus mimicking the early events of human periodontal disease (Figure 9, A and B). To determine whether this migration was associated with increased inflammation, we quantified the number of inflammatory cells and the area they occupied adjacent to the epithelium. The score for inflammation was the highest in the LPS + 6.3G9 antibody group representing approximately a twofold increase compared to water or LPS treatment alone (Figure 9C). The group treated with LPS + 7.8B3 also showed some inflammatory changes but significantly less than the LPS + 6.3G9 group (Figure 9C). Taken together, the rat model shows that blocking αvβ6 integrin-mediated TGF-β1 activation at the gingival crev-

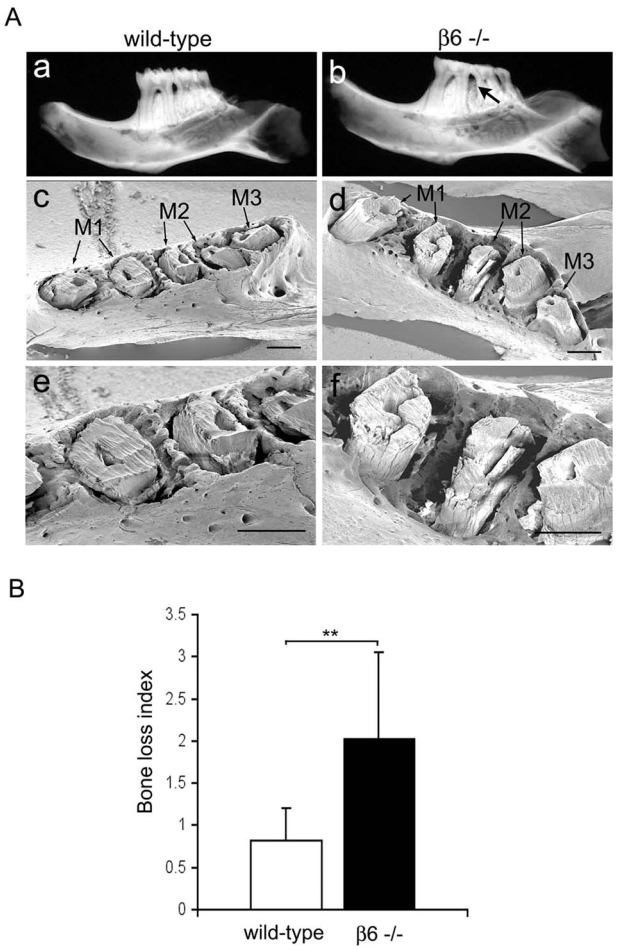

Figure 8. β6 integrin-knockout mice show extensive bone resorption between the teeth. **A:** Radiographs (**a**, **b**) and scanning electron microscopy images (**c–f**) of WT (**a**, **c**, **e**) and *Itgb6*$^{-/-}$ (β6$^{-/-}$; **b**, **d**, **f**) mouse half-mandibles from 12-month-old animals. The **arrow** in **b** points to an area of decreased bone density, indicating bone loss. In **c** and **d**, an interproximal resorption is noted between the first and second molars. M1, first molar; M2, second molar; M3, third molar. **B:** Quantitative assessment of the degree of bone loss measured from radiographs. Data presented are mean ± SD from 11 WT and 11 *Itgb6*$^{-/-}$ half-mandibles, providing 110 sites for measurement. The difference between WT and *Itgb6*$^{-/-}$ is statistically significant (**$P < 0.01$; Mann-Whitney *U*-test). Scale bars = 500 μm.

ice leads to histological alterations similar to those seen in early human periodontal disease.

Discussion

In the present study, we show for the first time that αvβ6 integrin is expressed in human and murine JE. This is also the first study showing that loss of a single gene in the JE can lead to the development of periodontal disease. Remarkably, a null-mutation for β6 integrin in mice caused all of the classic characteristics of spontaneous chronic inflammatory periodontal disease: apical migration of the pocket epithelium, inflammation, and advanced alveolar bone resorption. Our findings also indicate that the major protective role αvβ6 integrin plays against periodontal disease is via the activation of TGF-β1.

Considering its complex function in cell and immune regulation, TGF-β1 could function at multiple levels in periodontal protection. One could consider that the simplest explanations for the results of this study could be either epithelial adhesion deficiency directly caused by the lack of αvβ6 integrin or enhanced cell proliferation in the JE caused by altered TGF-β1 regulation of the cell cycle. In epithelial cells, αvβ6 mediates cell adhesion and migration on fibronectin and tenascin in collaboration with other integrins.[36,42,43] No known ligands of αvβ6 integrin have been found at the internal basal lamina between the tooth and the JE. Nor was there any evidence of the detachment of JE epithelial cells from tooth noticeable in the tissue sections except at the sites of pocket formation, indicating that cell adhesion to enamel and cementum was not affected in *Itgb6*$^{-/-}$ mice.

Inhibition of epithelial cell proliferation by TGF-β1 involves down-regulation of c-Myc, leading to the up-regulation of cyclin-dependent kinase inhibitors p15 and p21, which inhibit the CDK4/6-cyclin D- and CDK2-cyclin E-mediated phosphorylation of the retinoblastoma protein.[17,18] Enlarged JE attributable to increased cell proliferation in p21/p27 double-knockout mice supports the notion that TGF-β1 plays an important role in the regulation of JE proliferation.[44] However, no apical migration or inflammation was evident in these animals. Increased cell proliferation is a prerequisite for apical migration of JE in the *Itgb6*$^{-/-}$ mice during pocket formation. It is possible, therefore, that in the absence of αvβ6 integrin, cell proliferation is increased, contributing to the pocket formation. This is, however, unlikely a major reason for the periodontal disease observed in these mice.

It is well documented that bacteria, especially anaerobic microorganisms such as *P. gingivalis* in the periodontal pockets, contribute to periodontal disease.[37] Host response is believed to play a role in the modulation of progression of the disease.[45] Some recent evidence suggests, however, that the inflammation itself may be driving the process. In an animal model of periodontal disease, resolvin E1, which facilitates removal of leukocytes from the inflammatory site, can prevent pocket formation and bone loss despite the presence of anaerobic bacteria.[41] In clinical dentistry, an absence of inflammation in the gingiva has long been considered a good indicator of periodontal health, even in patients with a history of periodontal disease.[46] TGF-β1 plays a key role in the protection against acquired inflammatory conditions introduced by normal exposure to the environment. Mice deficient in TGF-β1 spontaneously develop mononuclear cell infiltrates in multiple organs with lethal consequences.[21,22] Although TGF-β1 can be activated by multiple mechanisms, an integrin-mediated pathway seems to dominate *in vivo* as evidenced by the observations that mice with RGE-mutated LAP show a phenotype similar to that of TGF-β1-null mice.[24] We report here that αvβ6 integrin-mediated activation of TGF-β1 also plays a crucial role in protection against inflammatory periodontal disease. The mechanism is likely to be complex, because TGF-β1 regulates inflammation at multiple levels. Shifting of leukocyte populations at various stages of periodontal disease further complicates the issue. Early periodontal le-

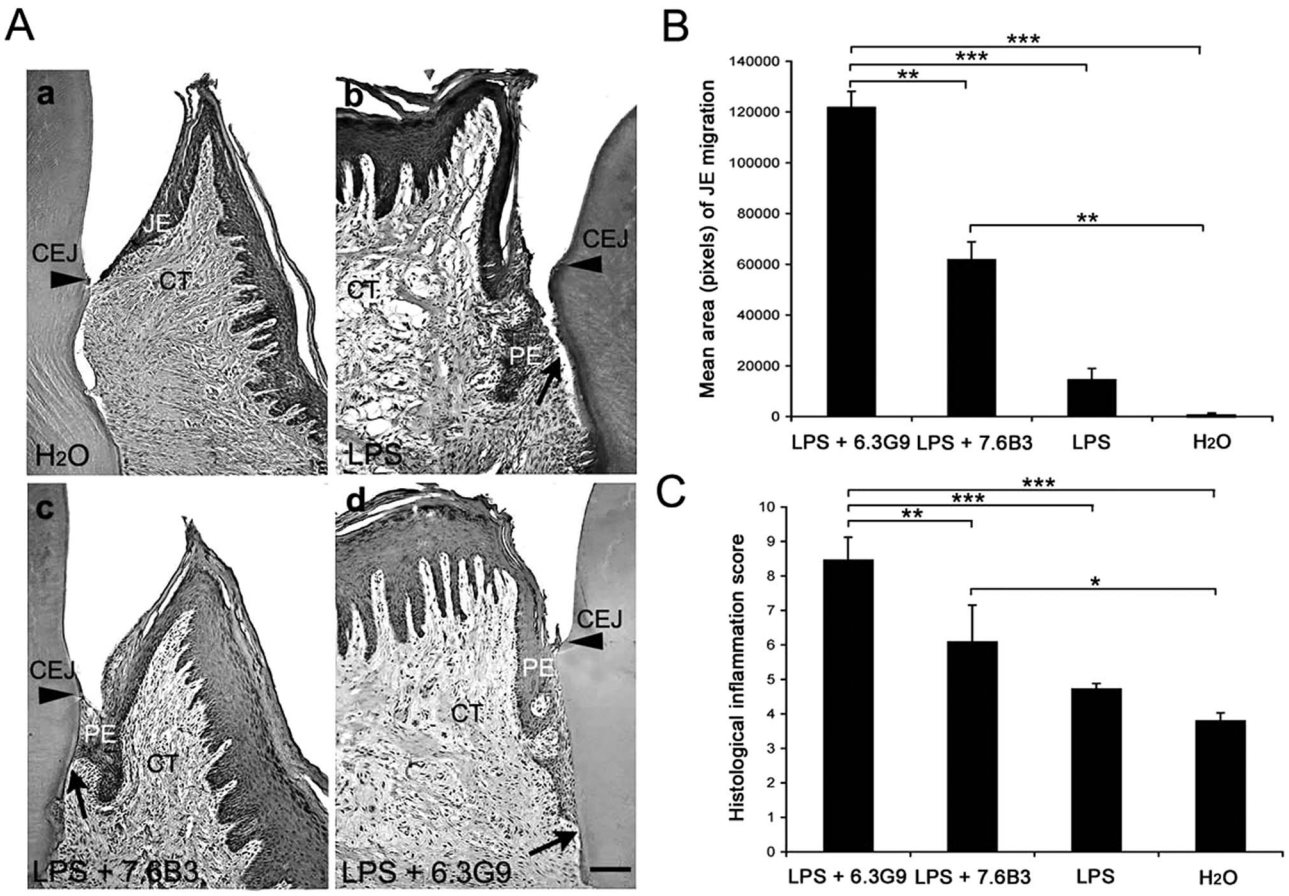

Figure 9. Blocking of αvβ6 integrin-mediated TGF-β1 activation increases apical epithelial migration and inflammation. **A:** H&E staining of rat gingiva treated daily with H_2O (**a**), LPS (**b**), LPS and a nonblocking anti-αvβ6 antibody (7.6B3, **c**) or LPS and an antibody that blocks αvβ6 integrin-mediated TGF-β1 activation (6.3G9, **d**) for 8 weeks. **Arrowheads** and **arrows** show the distance of epithelial migration. CT, connective tissue; PE, pocket epithelium. **B:** The epithelial migration was measured from 15 H&E-stained tissue sections from three rats in each treatment group. The results are presented as a mean area of migrated epithelium ± SD. **C:** The inflammatory infiltrate adjacent to the epithelium was quantified in H&E-stained sections using a combination index based on both the area occupied by inflammatory cells and the inflammatory cell density. The results are presented as mean score for inflammation ± SD. Only differences that were deemed statistically significant are indicated: $^*P < 0.05$; $^{**}P < 0.01$, $^{***}P < 0.001$ (analysis of variance and Tukey's post test). Scale bar = 200 μm.

sions contain mainly macrophages and T cells, whereas in progressive lesions, B cells dominate.[29] Proliferation, differentiation, and survival of T cells are all affected by TGF-β1.[20,47] TGF-β1 inhibits proliferation of naïve $CD4^+$ T cells and helper cell differentiation, but also regulates $CD8^+$ cells, B cells, macrophages, and even polymorphonuclear leukocytes.[20] The $CD4^+$ T cells are important targets for the TGF-β1-mediated regulation of inflammation.[48] A subpopulation of $CD4^+$ T cells called regulatory $CD4^+CD25^+FoxP3^+$ T cells may be especially important in TGF-β1-mediated suppression of inflammation.[19] The regulatory T cells infiltrate gingival tissue in periodontal disease, but lesions with bone resorption show reduced numbers of these cells, increased levels of IL-1β, and osteoclastogenic RANKL, suggesting that TGF-β1 signaling is affected in the active disease process.[49,50] Consistent with these findings, loss of TGF-β1-mediated suppression of T cells results in increased production of osteoclastogenic interferon-γ, TNF-α, and RANKL, and in bone loss.[51,52]

Although a role for keratinocytes in the immunoregulation of periodontal disease has been proposed, the specific functions of cell surface receptors and their ligands, such as αvβ6 integrin and TGF-β1, have not yet been investigated.[53] It is possible that keratinocytes serve as nonprofessional, antigen-presenting cells to the underlying lymphocytes in a process that is regulated by TGF-β1. In addition, keratinocytes may inhibit the proliferation of unprimed T cells via a TGF-β1-mediated mechanism.[54] Keratinocytes of the JE could also directly participate in the development of periodontal lesions by secreting a number of proinflammatory cytokines such as IL-1α, IL-1β, TNF-α, IL-6, and IL-8.[55,56] Exposure to LPS further increases the expression of these cytokines in the JE.[56] We show that TGF-β1 is strongly expressed in the JE and could serve as a counteracting cytokine toward those promoting inflammation. Using the rat model, we report that when TGF-β1 activation by αvβ6 integrin was suppressed in the JE, LPS enhanced both apical migration of the JE and inflammation, indicating that local disturbance in TGF-β1 signaling in the JE can cause the initial signs of periodontal disease. TSP-1 collaborates with αvβ6 integrin in TGF-β1 activation and suppression of lung and skin inflammation[23] but does not seem to participate in protection against spontaneous periodontal disease, because periodontal structures in β6 integrin,

thrombospondin-1, double-knockout mice were similar to those in the *Itgb6*$^{-/-}$ animals (unpublished results).

Interestingly, in human periodontal disease, the expression of $\alpha v\beta 6$ integrin was strongly down-regulated in epithelial cells that were surrounded by heavy inflammatory infiltrates of lymphocytes, thus mimicking acquired $\beta 6$ integrin deficiency. Although none of the proinflammatory cytokines tested in the study inhibited $\beta 6$ integrin expression in gingival keratinocytes, a treatment with LAP or a function-blocking anti-TGF-$\beta 1$ antibody strongly reduced it, showing that a significant part of $\alpha v\beta 6$ integrin expression in keratinocytes is maintained via endogenous TGF-$\beta 1$ production. Furthermore, a noncytolytic concentration of *P. gingivalis* extract effectively suppressed the stimulation of $\alpha v\beta 6$ integrin expression by TGF-$\beta 1$. The fact that heating the *P. gingivalis* whole cell lysate abolished this effect suggests a participation of proteinases. *P. gingivalis* is well known to produce large spectrum cysteine proteinases referred to as Arg- and Lys-gingipains, which are considered potential contributors to the pathogenic process of periodontal disease.[57] The reduced expression of keratinocyte cell surface $\alpha v\beta 6$ integrin caused by the *P. gingivalis* whole cell extract may result from the degradation of TGF-$\beta 1$ or the proteolysis/shedding of cell-associated $\alpha v\beta 6$ integrin similar to syndecan-1,[58] another important epithelial cell surface protein. *P. gingivalis* can adhere to keratinocytes and disturb the epithelial barrier.[59] Because TGF-$\beta 1$ is crucial for the maintenance of $\alpha v\beta 6$ integrin expression in keratinocytes and, inversely, $\alpha v\beta 6$ integrin is critical for TGF-$\beta 1$ activation, the presence of *P. gingivalis* in periodontal pockets in chronic periodontal disease could participate in the down-regulation of local TGF-$\beta 1$ signaling, $\alpha v\beta 6$ integrin expression, and consequent $\alpha v\beta 6$ integrin-mediated TGF-$\beta 1$ activation, leading to the exacerbated inflammation seen in periodontal disease. Other bacterial species may also participate in modulation of TGF-$\beta 1$ activation in the pocket epithelium. In mice lacking $\alpha v\beta 6$ integrin, normal oral flora could trigger the initiation of the disease process. Our study did not address the organisms present in the mouse periodontal lesions because bacteria associated with periodontal disease in mice are not well understood. Periodontal disease is relatively rare in laboratory mice because most mouse strains are resistant to it.[60] In the susceptible strains, the presentation of periodontal disease is very similar to human disease with chronic lesions with true pocket formation. The wild-type FVB mice used in this study exhibited some loss of tooth attachment with age because of normal eruption of teeth. True periodontal lesions were, however, not observed, and the JE remained at its normal position at CEJ. On the other hand, the lesions in the *Itgb6*$^{-/-}$ mice resembled closely those seen in human disease and also those described for susceptible strains of mice.[60] The molecular pathology of periodontal disease in *Itgb6*$^{-/-}$ mice mimics the inflammation found in the lungs and skin of these animals. This suggests that they all arise from the dysregulation of inflammation controlled by TGF-$\beta 1$.[23] Periodontal disease is associated with many other inflammatory conditions, and it is believed to contribute to the accumulated inflammatory burden in cardiovascular and joint diseases and also to affect pregnancy outcomes.[25,26] Acquired (bacteria-induced) loss of $\alpha v\beta 6$ integrin expression in JE in human periodontal disease may, therefore, have significant consequences in the overall health.

In conclusion, our data reveal that $\alpha v\beta 6$ integrin-mediated activation of TGF-$\beta 1$ plays a critical role in protecting against chronic inflammatory periodontal disease. The data further suggest that the epithelial cells drive the inflammatory process, which ultimately leads to bone resorption and tooth loss.

Acknowledgments

We thank Drs. Shelia M. Violette and Paul H. Weinreb for providing the $\alpha v\beta 6$ integrin antibodies, Drs. Dean Sheppard and Jack Lawler for kindly making available the $\beta 6$ integrin and TSP-1 knockout mice, and Mr. Cristian Sperantia for his excellent technical assistance.

References

1. Breuss JM, Gillett N, Lu L, Sheppard D, Pytela R: Restricted distribution of integrin $\beta 6$ mRNA in primate epithelial tissues. J Histochem Cytochem 1993, 41:1521–1527
2. Clark RA, Ashcroft GS, Spencer MJ, Larjava H, Ferguson MW: Re-epithelialization of normal human excisional wounds is associated with a switch from $\alpha v\beta 5$ to $\alpha v\beta 6$ integrins. Br J Dermatol 1996, 135:46–51
3. Haapasalmi K, Zhang K, Tonnesen M, Olerud J, Sheppard D, Salo T, Kramer R, Clark RA, Uitto VJ, Larjava H: Keratinocytes in human wounds express $\alpha v\beta 6$ integrin. J Invest Dermatol 1996, 106:42–48
4. Larjava H, Salo T, Haapasalmi K, Kramer H, Heino J: Expression of integrins and basement membrane components by wound keratinocytes. J Clin Invest 1993, 92:1425–1435
5. Hahm K, Lukashev ME, Luo Y, Yang WJ, Dolinski BM, Weinreb PH, Simon KJ, Chun Wang L, Leone DR, Lobb RR, McCrann DJ, Allaire NE, Horan GS, Fogo A, Kalluri R, Shield CF, III Sheppard D, Gardner HA, Violette SM: $\alpha v\beta 6$ integrin regulates renal fibrosis and inflammation in Alport mouse. Am J Pathol 2007, 170:110–125
6. Huang XZ, Wu JF, Cass D, Erle DJ, Corry D, Young SG, Farese RV Jr, Sheppard D: Inactivation of the integrin $\beta 6$ subunit gene reveals a role of epithelial integrins in regulating inflammation in the lung and skin. J Cell Biol 1996, 133:921–928
7. Chang H, Brown CW, Matzuk MM: Genetic analysis of the mammalian transforming growth factor-β superfamily. Endocr Rev 2002, 23:787–823
8. Verrecchia F, Mauviel A: Control of connective tissue gene expression by TGFβ: role of Smad proteins in fibrosis. Curr Rheumatol Rep 2002, 4:143–149
9. Taipale J, Miyazono K, Heldin CH, Keski-Oja J: Latent transforming growth factor-$\beta 1$ associates to fibroblast extracellular matrix via latent TGF-β binding protein. J Cell Biol 1994, 12:171–181
10. Flaumenhaft R, Abe M, Sato Y, Miyazono K, Harpel J, Heldin CH, Rifkin DB: Role of the latent TGF-β binding protein in the activation of latent TGF-β by co-cultures of endothelial and smooth muscle cells. J Cell Biol 1993, 120:995–1002
11. Nakajima Y, Miyazono K, Kato M, Takase M, Yamagishi T, Nakamura H: Extracellular fibrillar structure of latent TGF-β binding protein-1: role in TGF-β-dependent endothelial-mesenchymal transformation during endocardial cushion tissue formation in mouse embryonic heart. J Cell Biol 1997, 136:193–204
12. Gualandris A, Annes JP, Arese M, Noguera I, Jurukovski V, Rifkin DB: The latent transforming growth factor-β-binding protein-1 promotes in vitro differentiation of embryonic stem cells into endothelium. Mol Biol Cell 2000, 11:4295–4308
13. Munger S, Huang X, Kawakatsu H: The integrin $\alpha v\beta 6$ binds and activates latent TGF$\beta 1$: a mechanism for regulating pulmonary inflammation and fibrosis. Cell 1999, 96:319–328

14. Annes JP, Chen Y, Munger JS, Rifkin DB: Integrin αVβ6-mediated activation of latent TGF-β requires the latent TGF-β binding protein-1. J Cell Biol 2004, 165:723–734
15. Glick AB, Kulkarni AB, Tennenbaum T, Hennings H, Flanders KC, O'Reilly M, Sporn MB, Karlsson S, Yuspa SH: Loss of expression of transforming growth factor β in skin and skin tumors is associated with hyperproliferation and a high risk for malignant conversion. Proc Natl Acad Sci USA 1993, 90:6076–6080
16. Kane CJ, Knapp AM, Mansbridge JN, Hanawalt PC: Transforming growth factor-β1 localization in normal and psoriatic epidermal keratinocytes in situ. J Cell Physiol 1990, 144:144–150
17. Robson CN, Gnanapragasam V, Byrne RL, Collins AT, Neal DE: Transforming growth factor-β1 up-regulates p15, p21 and p27 and blocks cell cycling in G1 in human prostate epithelium. J Endocrinol 1999, 160:257–266
18. Ten Dijke P, Goumans MJ, Itoh F, Itoh S: Regulation of cell proliferation by Smad proteins. J Cell Physiol 2002, 191:1–16
19. Wahl SM, Swisher J, McCartney-Francis N, Chen W: TGF-β: the perpetrator of immune suppression by regulatory T cells and suicidal T cells. J Leukoc Biol 2004, 76:15–24
20. Li MO, Sanjabi S, Flavell RA: Transforming growth factor-β controls development, homeostasis, and tolerance of T cells by regulatory T cell-dependent and -independent mechanisms. Immunity 2006, 25: 455–471
21. Shull MM, Ormsby I, Kier AB, Pawlowski S, Diebold RJ, Yin M, Allen R, Sidman C, Proetzel G, Calvin D, Annunziata N, Doetschman T: Targeted disruption of the mouse transforming growth factor-β1 gene results in multifocal inflammatory disease. Nature 1992, 359:693–699
22. Kulkarni AB, Huh CG, Becker D, Geiser A, Lyght M, Flanders KC, Roberts AB, Sporn MB, Ward JM, Karlsson S: Transforming growth factor β1 null mutation in mice causes excessive inflammatory response and early death. Proc Natl Acad Sci USA 1993, 90: 770–774
23. Ludlow A, Yee KO, Lipman R, Bronson R, Weinreb P, Huang X, Sheppard D, Lawler J: Characterization of integrin β6 and thrombospondin-1 double-null mice. J Cell Mol Med 2005, 9:421–437
24. Yang Z, Mu Z, Dabovic B, Jurukovski V, Yu D, Sung J, Xiong X, Munger JS: Absence of integrin-mediated TGFβ1 activation in vivo recapitulates the phenotype of TGFβ-null mice. J Cell Biol 2007, 176:787–793
25. Meurman JH, Sanz M, Janket SJ: Oral health, atherosclerosis, and cardiovascular disease. Crit Rev Oral Biol Med 2004, 15:403-413
26. Pussinen PJ, Mattila K: Periodontal infections and atherosclerosis: mere associations? Curr Opin Lipidol 2004, 15:583–588
27. Schroeder HE, Listgarten MA: The gingival tissues: the architecture of periodontal protection. Periodontology 2000 1997, 13:91–120
28. Bosshardt DD, Lang NP: The junctional epithelium: from health to disease. J Dent Res 2005, 84:9–20
29. Gemmell E, Seymour GJ: Immunoregulatory control of Th1/Th2 cytokine profiles in periodontal disease. Periodontology 2000 2004, 35:21–41
30. Weinreb PH, Simon KJ, Rayhorn P, Yang WJ, Leone DR, Dolinski BM, Pearse BR, Yokota Y, Kawakatsu H, Atakilit A, Sheppard D, Violette SM: Function-blocking integrin αvβ6 monoclonal antibodies: distinct ligand-mimetic and nonligand-mimetic classes. J Biol Chem 2004, 279:17875–17887
31. Huang X, Wu J, Zhu W, Pytela R, Sheppard D: Expression of the human integrin β6 subunit in alveolar type II cells and bronchiolar epithelial cells reverses lung inflammation in β6 knockout mice. Am J Respir Cell Mol Biol 1998, 19:636–642
32. Larjava H, Lyons JG, Salo T, Mäkelä M, Koivisto L, Birkedal-Hansen H, Akiyama SK, Yamada KM, Heino J: Anti-integrin antibodies induce type IV collagenase expression in keratinocytes. J Cell Physiol 1993, 157:190–200
33. Grenier D: Degradation of host protease inhibitors and activation of plasminogen by proteolytic enzymes from Porphyromonas gingivalis and Treponema denticola. Microbiology 1996, 142:955–961
34. Darveau RP, Hancock RE: Procedure for isolation of bacterial lipopolysaccharides from both smooth and rough Pseudomonas aeruginosa and Salmonella typhimurium strains. J Bacteriol 1983, 155: 831–838
35. Mäkelä M, Salo T, Larjava H: MMP-9 from TNFα-stimulated keratinocytes binds to cell membranes and type I collagen: a cause for extended matrix degradation in inflammation? Biochem Biophys Res Commun 1998, 253:325–335
36. Koivisto L, Larjava K, Häkkinen L, Uitto VJ, Heino J, Larjava H: Different integrins mediate cell spreading, haptotaxis and lateral migration of HaCaT keratinocytes on fibronectin. Cell Adhes Commun 1999, 7:245–257
37. Holt SC, Ebersole JL: Porphyromonas gingivalis, Treponema denticola, and Tannerella forsythia: the "red complex", a prototype polybacterial pathogenic consortium in periodontitis. Periodontology 2000 2005, 38:72–122
38. Sorsa T, Tjäderhane L, Konttinen YT, Lauhio A, Salo T, Lee HM, Golub LM, Brown DL, Mäntylä P: Matrix metalloproteinases: contribution to pathogenesis, diagnosis and treatment of periodontal inflammation. Ann Med 2006, 38:306–321
39. Takata T, Miyauchi M, Ogawa I, Ito H, Kobayashi J, Nikai H: Reactive change in proliferative activity of the junctional epithelium after topical application of lipopolysaccharide. J Periodontol 1997, 68:531–535
40. Ekuni D, Yamamoto T, Yamanaka R, Tachibana K, Watanabe T: Proteases augment the effects of lipopolysaccharide in rat gingiva. J Periodontal Res 2003, 38:591–596
41. Hasturk H, Kantarci A, Ohira T, Arita M, Ebrahimi N, Chiang N, Petasis NA, Levy BD, Serhan CN, Van Dyke TE: RvE1 protects from local inflammation and osteoclast-mediated bone destruction in periodontitis. FASEB J 2006, 20:401–403
42. Huang X, Wu J, Spong S, Sheppard D: The integrin αvβ6 is critical for keratinocyte migration on both its known ligand, fibronectin, and on vitronectin. J Cell Sci 1998, 111:2189–2195
43. Koivisto L, Grenman R, Heino J, Larjava H: Integrins α5β1, αvβ1, and αvβ6 collaborate in squamous carcinoma cell spreading and migration on fibronectin. Exp Cell Res 2000, 255:10–17
44. Watanabe K, Petro BJ, Sevandal M, Anshuman S, Jovanovic A, Tyner AL: Histochemical examination of periodontal junctional epithelium in p21/p27 double knockout mice. Eur J Oral Sci 2004, 112:253–258
45. Kantarci A, Hasturk H, Van Dyke TE: Host-mediated resolution of inflammation in periodontal diseases. Periodontology 2000 2006, 40:144–163
46. Lang NP, Adler R, Joss A, Nyman S: Absence of bleeding on probing. An indicator of periodontal stability. J Clin Periodontol 1990, 17:714–721
47. Gorelik L, Flavell RA: Transforming growth factor-β in T-cell biology. Nat Rev Immunol 2002, 2:46–53
48. Rudner LA, Lin JT, Park IK, Cates JM, Dyer DA, Franz DM, French MA, Duncan EM, White HD, Gorham JD: Necroinflammatory liver disease in BALB/c background. TGF-β1-deficient mice requires CD4+ T cells. J Immunol 2003, 170:4785–4792
49. Nakajima T, Ueki-Maruyama K, Oda T, Ohsawa Y, Ito H, Seymour GJ, Yamazaki K: Regulatory T-cells infiltrate periodontal disease tissues. J Dent Res 2005, 84:639–643
50. Ernst CW, Lee JE, Nakanishi T, Karimbux NY, Rezende TM, Stashenko P, Seki M, Taubman MA, Kawai T: Diminished forkhead box P3/CD25 double-positive T regulatory cells are associated with the increased nuclear factor-κB ligand (RANKL+) T cells in bone resorption lesion of periodontal disease. Clin Exp Immunol 2007, 148:271–280
51. Gao Y, Qian WP, Dark K, Toraldo G, Lin AS, Guldberg RE, Flavell RA, Weitzmann MN, Pacifici R: Estrogen prevents bone loss through transforming growth factor β signaling in T cells. Proc Natl Acad Sci USA 2004, 101:16618–16623
52. Gao Y, Grassi F, Ryan MR, Terauchi M, Page K, Yang X, Weitzmann MN, Pacifici R: IFNγ stimulates osteoclast formation and bone loss in vivo via antigen-driven T cell activation. J Clin Invest 2007, 117: 122–132
53. Suchett-Kaye G, Morrier JJ, Barsotti O: Interactions between non-immune host cells and the immune system during periodontal disease: role of the gingival keratinocyte. Crit Rev Oral Biol Med 1998, 9:292–305
54. Laning JC, Isaacs CM, Hardin-Young J: Normal human keratinocytes inhibit the proliferation of unprimed T cells by TGFβ and PGE2, but not IL-10. Cell Immunol 1997, 175:16–24
55. Tonetti MS, Imboden MA, Lang NP: Neutrophil migration into the gingival sulcus is associated with transepithelial gradients of interleukin-8 and ICAM-1. J Periodontol 1998, 69:1139–1147

56. Miyauchi M, Sato S, Kitagawa S, Hiraoka M, Kudo Y, Ogawa I, Zhao M, Takata T: Cytokine expression in rat molar gingival periodontal tissues after topical application of lipopolysaccharide. Histochem Cell Biol 2001, 116:57–62
57. Imamura T: The role of gingipains in the pathogenesis of periodontal disease. J Periodontol 2003, 74:111–118
58. Andrian E, Grenier D, Rouabhia M: Porphyromonas gingivalis gingipains mediate the shedding of syndecan-1 from the surface of gingival epithelial cells. Oral Microbiol Immunol 2006, 21:123–128
59. Sandros J, Papapanou P, Dahlen G: Porphyromonas gingivalis invades oral epithelial cells in vitro. J Periodontal Res 1993, 28:219–226
60. Page RC, Schroeder HE: Periodontitis in Man and Other Animals. A Comparative Review. Basel, Karger, 1982